AIAA JOURNAL
Vol. 46, No. 1, January 2008

# Reliability-Based Design of a Slat-Track Fatigue Life Using Mesh Morphing Technology

Roberto d'Ippolito* and Stijn Donders†
*LMS International, 3001 Leuven, Belgium*
Michael Hack‡
*LMS Deutschland GmbH, 67657 Kaiserslautern, Germany*
Geert Van der Linden§
*ASCO Industries, 1930 Zaventem, Belgium*
and
Dirk Vandepitte¶ and David Moens**
*Katholieke Universiteit Leuven, 3001 Heverlee, Belgium*

DOI: 10.2514/1.29686

**Although the aerospace production process is much better controlled than in other industries, it remains true that very small manufacturing tolerances exist in the geometrical parameters such as flange thickness and hole diameters. In the current design process, the effect of this manufacturing variability on the structural durability and safety cannot be accurately assessed and is hence compensated for by applying safety factors. This is not an ideal situation, because it may lead to slightly overdesigned structures. A much more promising approach is to include probabilistic models of design variables into the mechanical simulation process. With a new methodology based on reliability analysis, engineers can obtain a better understanding of the actual effect of the manufacturing tolerances and of variability in material properties. Based on the analysis results, the robustness and reliability of the design can be assessed and improved if needed. In this paper, the aforementioned probabilistic approach is demonstrated on a slat-track structure. Measurements of different geometrical properties were collected during the manufacturing process and their variability was characterized probabilistically with statistical models. Then a reliability analysis was carried out using mesh morphing technology and fatigue life predictions with an industrial-sized finite element model of the slat track to assess the reliability of the structure in terms of fatigue life. The outcome of the analysis consists of a probabilistic model of the structural performance (e.g., fatigue life for the slat track), given the variability in the geometrical parameters. Then a reliability-based design optimization procedure was carried out to improve the design of the slat track while maintaining the same reliability of the nominal design.**

## Nomenclature

$B_j$ = $j$th basis of functions
$G$ = performance function
$L$ = axial beam force acting on the slat track
$M_B$ = bending moment
$M_P$ = moment of the pinion acting on the inner rack of the slat track
$N$ = number of samples in a population
$P_f$ = probability of failure
$\alpha_j$ = $j$th function coefficient
$\beta$ = reliability index
$\beta_t$ = target reliability index
$\gamma_{SS}$ = slat-track extension angle
$\rho_{AB}$ = linear correlation coefficient between two populations $A$ and $B$
$\hat{\rho}_{AB}$ = estimator of the linear correlation coefficient between two populations $A$ and $B$
$\sigma$ = standard deviation
$\Phi$ = standard normal cumulative distribution function

Presented as Paper 2153 at the 47th AIAA/ASME/ASCE/AHS/ASC Structures, Structural Dynamics, and Materials Conference, Newport, RI, 1–4 May 2006; received 10 January 2007; revision received 31 August 2007; accepted for publication 9 September 2007. 

*Research Engineer, Computer-Aided Engineering Division. Student Member AIAA.
†Research Engineer, Computer-Aided Engineering Division.
‡Product Manager Durability Computer-Aided Engineering.
§Research & Development Engineer.
¶Professor, Department of Mechanical Engineering, Division of Production Engineering, Machine Design and Automation, Kasteelpark Arenberg 41. Senior Member AIAA.
**Ph.D., Department of Mechanical Engineering, Division Division of Production Engineering, Machine Design and Automation, Kasteelpark Arenberg 41. Member AIAA.

## I. Introduction

CURRENTLY, aerospace industries are dedicating much attention to improve product quality and reliability through a virtual simulation environment. Product designers worldwide are confronted with highly competitive though conflicting demands to deliver more complex products with increased quality in ever-shorter development cycles. Optimizing design performance with purely test-based approaches is no longer an option, and numerical simulation methods are widely used to model, assess, and improve the product design based on virtual prototypes. Functional performance attributes such as body strength; noise, vibration, and harshness (NVH); vibroacoustic modeling (VAM); durability; and crashworthiness [1–3] can already be optimized before entering the expensive test phase. A new paradigm of mechanical testing as an essential enabler in the virtual prototype optimization process resulted. Combined advances in test and simulation push the design envelope to shorter and higher-quality product development cycles [4].

A major issue in the use of virtual prototypes is the presence of uncertainty and variability [5] in the material and geometrical properties and manufacturing processes [6] as well as in applied loads; their effect on the performance cannot be predicted from a single finite element (FE) analysis [7,8]. A traditional solution is to

apply safety factors on the system parameters, but this typically leads to oversized, too-heavy structures. A more promising approach is to include uncertainty in the mechanical simulation process, thus assessing and improving the reliability of the design. In fact, in real-life structures it is typically not possible to assign an exact value to all parameters [6].

Oberkampf et al. [5] distinguished two classes of nondeterminism in parameter values. Variability refers to the variation inherent to the physical system or the environment under consideration, and uncertainty is a potential deficiency in any phase or activity of the modeling process that is due to lack of knowledge. Note that other definitions may be agreed upon, but the preceding definitions are used throughout this paper. Variability (material characteristics, manufacturing tolerances, etc.) can be handled with a probabilistic approach, and uncertainty (damping, boundary conditions, etc.) can be assessed with a possibilistic approach (e.g., fuzzy arithmetic).

In this paper, a fatigue analysis of a slat track using a validated FE model is considered, because it is representative of a field in which a better understanding of the effect of variability is required. In fact, for this model, a probabilistic characterization of the variability was introduced in the computer-aided engineering process using advanced mesh morphing technologies. Based on this improved simulation environment, a statistical characterization of the fatigue performance of the structure was assessed. In this way, the new probabilistic information gathered from the production process and introduced in the simulation environment allows the design engineer to obtain a better understanding of the actual effect of the manufacturing tolerances on structural safety. In this context, variability quantification was carried out to enable the application of the probabilistic techniques available for reliability-based design [9,10]. These techniques, developed in the last 30 years for a number of different cases, allow the characterization of variability in structural parameters (geometry, material properties, etc.) and the analysis of its propagation on the final response of the structure or system [11]. This effect can be studied using reliability analysis and reliability-based design optimization strategies that make use of limit-state approximations as well as of sampling procedures, thus giving the analyst the ability to balance the accuracy and the computational effort required to extract the necessary information on safety and performance stability. Moreover, a reliability-based design optimization procedure was carried out to improve the design of the slat track by minimizing the total mass while maintaining the same reliability level of the nominal design.

Although reliability-based optimization methodologies have been applied in many structural analysis fields [12], also taking into account many failure modes and optimization strategies, one of the main problems that had to be faced was a consistent definition of the variability inherent to the design parameters selected. In this paper, the probabilistic characterization of this variability was based on real data collected during the manufacturing process of the slat-track component, and thus no assumption or expert opinion on the distribution type for each parameter was used. In this way, the results are minimally affected by the probabilistic modeling of the design variables, and only bounded by the range of validity of the finite element method theory and by the damage accumulation procedure used for fatigue life prediction.

The presented methodologies are being studied and developed in the context of the EC Research Training Network (RTN) MADUSE[††] and the Instituut voor Innovatie door Wetenschap en Technologie (IWT) research and development project combining testing and simulation to improve the reliability of safety-critical airplane components.

## II. Analysis Case: Slat Track

The FE core model (Fig. 1b) consists of 236,630 tetrahedral elements generated by an automated mesh generator. Beam elements were added to correctly represent the rack in the inner section of the slat-track profile and to model the rod-leading-edge assembly, connected by ball bearings.

The slat track is made of a 18% nickel–cobalt–molybdenum maraging steel, which has an ultimate tensile strength equal to 1800 MPa and Young's modulus of 184 GPa.

### A. Measured Data and Probabilistic Characterization

Probabilistic analysis requires that a representative set of data is available to characterize the geometrical variabilities of the manufacturing process. Because every manufacturing process is different from the other, there are no standard assumptions that can be made on the type of distribution to be used to characterize geometric tolerances. This is, of course, not the case for physical quantities such as material properties, which can be easily modeled and for which well-known guidelines are available for a wide class of materials.

For the slat track, four input parameters were selected for the probabilistic characterization, as demonstrated in Fig. 1a. For these parameters, geometrical measurements were taken on 1573 specimens of nominally identical slat tracks during the manufacturing process and on both sides of the slat-track dimensions. In particular, the difference between the nominal (design) value and the actual value was measured for each parameter. These data were then used to build a probabilistic characterization of the input parameters using random variables. For this purpose, a least-squares fitting procedure was used with the four available sets of data to find the best statistical distributions that represent the population of measured differences. The type of distribution and its mean and standard deviations are reported in Table 1. The distribution models were verified with a $\chi^2$ hypothesis test [13], which checks that the selected model is representative of the data set used for the least-squares procedure.

A check on the statistical correlation of the design parameters was also carried out using the data acquired during the manufacturing process. This check needs to be performed to avoid a possible assumption of statistical independency affecting the simulation results. Thus, the estimation $\hat{\rho}_{AB}$ of the linear correlation coefficient $\rho_{AB}$ between two generic data sets $A$ and $B$ was carried out for the input parameters considered in this case. The definition of the approximate linear correlation coefficient $\hat{\rho}_{AB}$ of $N$ samples each is (in the least-squares sense [14])

$$\hat{\rho}_{AB} = \frac{\hat{\mathrm{cov}}\{A,B\}}{\sqrt{\hat{\mathrm{var}}\{A\}\hat{V}ar\{B\}}} = \frac{\frac{1}{N}\sum_{i=1}^{N}(a_i b_i) - \mu_A \mu_B}{\sqrt{(\frac{1}{N}\sum_{i=1}^{N} a_i^2 - \mu_A^2)(\frac{1}{N}\sum_{i=1}^{N} b_i^2 - \mu_B^2)}}$$

where $\hat{\mathrm{cov}}\{A,B\}$ is the approximate covariance estimated using the realizations of the two random variables, and $\hat{\mathrm{var}}\{A\}$ and $\hat{\mathrm{var}}\{B\}$ are the approximate variances estimated using the realizations of the two random variables.

In Table 2, the values of the approximate correlation coefficients for the design parameters of Table 1 are reported (correlation matrix).

As can be seen from the correlation matrix, most of the parameters have little or no correlation, except between the difference-base-height and the difference-top-height parameters, which show a negative correlation. The causes of this correlation were not investigated, because they mainly depend on the manufacturing tool used for the slat-track production, but their effect was taken into account during the reliability computations. More details will be given in the Results section. In Fig. 2, the correlation plots for all the parameters are reported. The presence of a few outlier samples (defined as observations that are far from the mass data of values in a statistical population of samples) was neglected for the computation of the correlation matrix. Various methods exist to classify an observation as an outlier (see [13] for further details).

### B. Objective of the Analysis

In this paper, the presence of variability in the input parameters was taken into account to analyze the fatigue life of the slat track using the FE model. The propagation of variability in the structural analysis and its effect on the component performance was analyzed, and an optimization procedure based on the obtained results was

[††]Data available online at http://www.maduse.org/ [retrieved 1 October 2007].

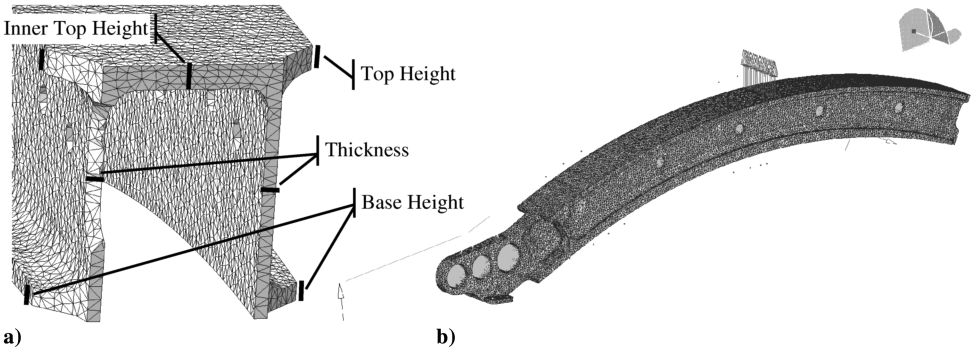


**Fig. 1 Slat-track FE model with loads and constraints.**

carried out to improve the weight of the structure, reducing the total mass while keeping the same reliability level. The statistical characterization of the input parameters and their measured correlation was used in the computation of the fatigue life, thus allowing the application of reliability analysis and reliability-based design optimization (RBDO) techniques using probabilistic constraint formulations. Details on these well-assessed reliability-based techniques and their limitations can be found in [9,10,15–28].

Note that the number of variables and their selection is not limited to the present choice, because they can be changed and increased in number, depending on the particular application. In fact, it is the engineer who should ensure that all relevant tolerance parameters are included in the analysis. Also, a number of techniques are available to handle high-dimensional and nonlinear problems, in which the number of parameters cannot be reduced reasonably without negligible approximations [21].

For the present case, focus was given only to geometrical quantities and not to other sources of variability (e.g., loads, material properties, etc.). This does not affect the general applicability of the reliability techniques described in this paper. This choice is mainly motivated by the amount of data available for the characterization of the geometrical tolerances, whereas for other sources of variability, either not enough data were available (e.g., for loads) or the inherent variability had a negligible effect on the structural response because variability is better controlled in other processes (e.g., material properties).

## III. Considerations on Using the Finite Element Method

In this paper, the word *physical* refers to the used FE model and to the particular characterization of the variability of the input parameters, including their boundaries. In fact, when using FE models to represent reality, at least three processes should be carried out, as stated by the Technical Committee on Model Credibility of the Society for Computer Simulation in 1979, as stated in [29]. This process, shown in Fig. 3, identifies the primary phases and activities of modeling and simulation, including model verification and validation.

As defined by the AIAA verification and validation guide [30], verification is the process of determining that a model implementation accurately represents the developer's conceptual description of the model and the solution to the model, and validation is the process of determining the degree to which a model is an accurate representation of the real world from the perspective of the intended uses of the model. These definitions imply that the FE model cannot be used with any possible combination of the input parameters, disregarding the domain of verification and validation of the model itself. Unfortunately, the boundaries of the domain of possible computations are unknown or extremely difficult to be assessed correctly. The assumption of an unbounded stochastic space, which till now has often been accepted in literature, is typically not valid for FE computations. Also, there is an unknown error in the probability of failure $P_f$ estimation that is due to the definition of the domain itself, especially when using non-Gaussian random variables.

In this paper, the aforementioned problem was simplified for engineering practice: the input parameters were bounded inside a hypercube centered in the origin with an edge size varying from 10 to $30\sigma$, depending on the values of the input parameters' scatter. This keeps the reliability analysis algorithms inside the region that can be explored by the finite element method with a verified and validated model. For example, in the case of a $20\sigma$ edge hypercube, the nearest boundary is located at $10\sigma$ from the origin, which corresponds to a failure probability of less than $2.0 \times 10^{-23}$. It could also be the case that the nearest point lies outside the hypercube of $20\sigma$; in that case, it is guaranteed that the reliability index is higher than $10\sigma$, which is sufficient for all practical purposes because quality control processes could reject components with a deviation from a nominal value greater than $10\sigma$.

**Table 1 Statistical characterization of the input parameters, based on measured data**

| Variable | Design value | Distribution | Mean of difference from nominal | Standard deviation of difference from nominal |
|---|---|---|---|---|
| Difference base height | Undisclosed | Normal | 0.15181 mm | 0.05918 mm |
| Difference thickness | Undisclosed | Normal | 0.14722 mm | 0.04942 mm |
| Difference top height | Undisclosed | Normal | 0.02503 mm | 0.07012 mm |
| Difference inner top height | Undisclosed | Normal | 0.10272 mm | 0.06084 mm |

**Table 2 Statistical correlation between the input parameters, based on measured data**

| | Difference base height | Difference thickness | Difference top height | Difference inner top height |
|---|---|---|---|---|
| Difference base height | 1 | 0.0944 | −0.4679 | −0.1123 |
| Difference thickness | 0.0944 | 1 | −0.1774 | 0.0563 |
| Difference top height | −0.4679 | −0.1774 | 1 | 0.1694 |
| Difference inner top height | −0.1123 | 0.0563 | 0.1694 | 1 |

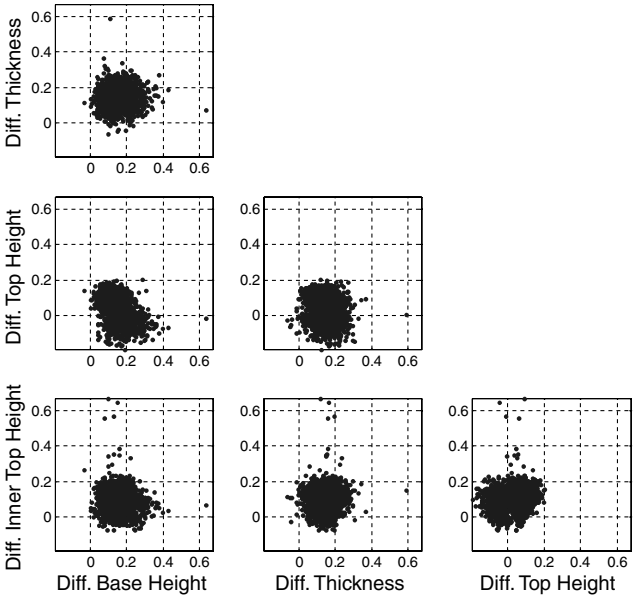


**Fig. 2 Correlation plots for the design parameters.**

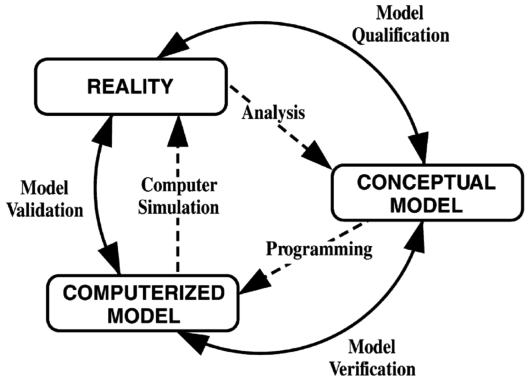




**Fig. 3 View of modeling and simulation by the Society for Computer Simulation.**

## IV. Analysis Case Implementation

With the variability introduced in the input parameters, a first estimation of the reliability of the nominal design is made. This allows the estimation of the degree of conservatism for the nominal design and how much it can be improved without violating the target reliability level. Then the performance behavior of the FE model was observed and an RBDO process was applied to optimize the design by reducing the total mass while satisfying the following probabilistic constraint:

$$\beta_t = 6 \Rightarrow P_f = 9.86 \times 10^{-10} \tag{1}$$

To perform the RBDO procedure, a software code was developed and used. The optimization process is managed by an OPTIMUS [31] thread that determines the necessary steps to reach the optimum design point that satisfies the probabilistic constraint of Eq. (1), using a sequential quadratic programming (SQP) approach. Note that the optimization process is a deterministic process with a probabilistic constraint. Thus, the result is an optimum point that is also reliable with respect to the required failure probability.

For each iteration of the optimization process, the algorithm requires the evaluation of the performance function at specific values of the input parameters, so that a static FE analysis has to be performed for each evaluation. To accomplish this task, another process-management thread was created that submits the new problem to the FE solver and extracts the necessary results.

The fatigue analysis of the slat track requires the integration of different procedures. Given a material degradation model, a standard durability assessment usually requires one structural analysis with unit loads together with the simulation of the repetition of the selected load history for a number of cycles. Further details will be given in Sec. IV.B.

For the present case, another step is required before the structural analysis can be performed. In fact, to take into account the variability of the input parameters, a transformation of the mesh is required. This transformation turns the nominal mesh into a morphed mesh, for which the values of the geometric input parameters are different from those of the nominal design. This morphed mesh can better represent the real product, without the necessity of remeshing from the CAD geometry. Thus, the slat-track mesh first needs to be modified to reflect the new input parameter configuration and then analyzed with unit loads using a FE solver. The results of the structural analysis are then used for the durability simulation. The outcome of the fatigue analysis, in terms of safety factor, can finally be used for the performance function of the slat track.

### A. Mesh Morphing

The type of mesh transformation called mesh morphing [32] consists of a change in the position of the nodes belonging to a specified mesh, following a given expression. This expression can be mathematical, such as a matrix, or geometrical (for example, the definition of a target shape). The morphing technology offers very interesting perspectives to apply such mesh modifications in a user-friendly and application-oriented way [33]. The most commonly used mesh morphing techniques are *free-form morphing* and *control-based approach*.

In free-form morphing, a set of morphing tools acts directly on the mesh. The approach uses the concept of control nodes, deformable nodes, and fixed nodes. Fixed nodes determine the boundary of the area of the deformable zone of the mesh. The deformable nodes correspond to the nodes that will be morphed. The actual displacement of the deformable nodes is determined by the displacement of the control nodes. To move the control nodes, several transformations can be applied, including projection (to surfaces or lines), translation, rotation, alignment, and scaling.

In a control-based approach, morphing operations are not carried out directly on the mesh of the existing FE model. Instead, morphing is applied by means of control blocks. Each control block represents a volume that envelops a small part of the existing FE mesh. By linking the location of the FE nodes inside each control block to the location of the corners of the control block, morphing operations applied to the blocks automatically define the geometry of the morphed FE model.

For the case considered in this paper, the first approach was selected. The particular complexity of the mesh made the use of control blocks less suitable. In particular, referring to Fig. 1, four different free-form morphing setups were created, one for each input parameter. Each setup has a set of control, deformable, and fixed nodes and can share nodes with other setups, thus allowing overlapping (or cumulative) transformations. In this case, the presence of overlapping mesh morphing transformations might lead to a degradation of the quality of some finite elements. For this reason, a sequence of application of the four transformations was identified that minimizes the possible distortion of the geometry of the finite elements involved in the transformation and guarantees a sufficient element quality level for the deformed mesh. As a consequence, the well-known problem of the distortion for elements at the junction between deformed and undeformed mesh has a negligible effect.

The morphing process has to be repeated a number of times for each combination of the input parameters. The performance function needs to be evaluated for each set of mesh morphing transformations, thus requiring a durability analysis each time.

### B. Durability Analysis

Because fatigue is the degradation of a material due to repeated cyclic loading, this typically means that for metals, there is an initiation of small cracks from active slip bands in grains on the free surface of a specimen, component, or structure. These small cracks eventually link to form large cracks that either break or severely degrade the performance of a component. Also, when repeated fatigue life tests are performed, one does not find exactly repeated results, but rather a scattered set of results. There are natural variations in material properties, component dimensions, customer service loads, and manufacturing tolerances. Probabilistic distributions can be used to characterize the variation of these variables and include this variability in the design process. This better explains and predicts the scatter obtained in fatigue test results. Two basic approaches were developed to estimate the crack-initiation life of components and to address fatigue analysis and design for durability: the stress-life approach and the strain-life approach. The goal of both approaches is to estimate the crack-initiation life of structures by combining a mechanics-based analysis of stresses or strains with the results of basic material property tests. For the present case, the strain-life approach was selected and the cyclic stress–strain curve and the strain-life curve were determined using the uniform material law [34]. Further details on the validation of the uniform material law model can be found in [35].

For the slat track, in-flight measured data were used for the fatigue analysis [35]. The aircraft was instrumented as for the normal qualification test campaign, for which several different measurements are usually acquired in many different flight conditions. From this large database, a subset of measuring channels was selected to retrieve the measurements of interest for the fatigue assessment on the slat track. All significant flight conditions were identified on the selected channels and the necessary data were extracted. This represents a reliable base for the fatigue life prediction.

In particular, all loads acting on the slat track were measured at three locations (Fig. 4). The acquisition and recording of the bending moment $M_B$ and of the axial beam force $L$ was done by using strain gauges at these locations. Also, the moment $M_P$ of the pinion acting on a rack at the inner side of the slat track was measured at different positions, depending on the slat-setting angle $\gamma_{SS}$. For the present case, the most critical condition was identified when the slat track was extended with an angle of $\gamma_{SS} = 20$ deg. An extensive analysis of the fatigue performance of the slat track is reported in [35].

The durability performance of the slat track was expressed in terms of a safety factor. The safety factor is always defined as the factor that can be multiplied to the loads to reach the endurance limit (infinite life) with respect to the amplitude of the largest stress cycle. For example, a safety factor of 2 means that the load does not cause any cyclic damage accumulation as long as it is scaled with a factor less than 2. Damage accumulation for high- or low-cycle fatigue failure starts when the factor is greater than 2.

In this paper, the minimum safety factor on the FE model was considered as representative of the fatigue performance of the slat track. The element for which the minimum safety factor is computed will be called a "hot spot" and can change depending on the variation of the input parameters. Further details are given in Sec. V.A.

### C. Process Integration

To automate the whole procedure, a process integration setup was created. The integration was divided in two steps: integration of the mesh morphing/durability analysis and the creation of the necessary input and output files needed for the analysis. The first part was accomplished by using LMS Virtual.Lab [36] together with a Visual Basic Application script. This block was integrated in an OPTIMUS graph, providing the necessary problem definition, input/output files, results extraction, and postprocessing.

Because the computational effort for the whole process can be considerable for industrial FE models, a design-of-experiments [37] (DOE) approach was selected to limit the time needed. A Latin hypercube DOE in the range of $-15\sigma$ to $+15\sigma$ was used to compute the performance of the structure in 80 points. This range was chosen

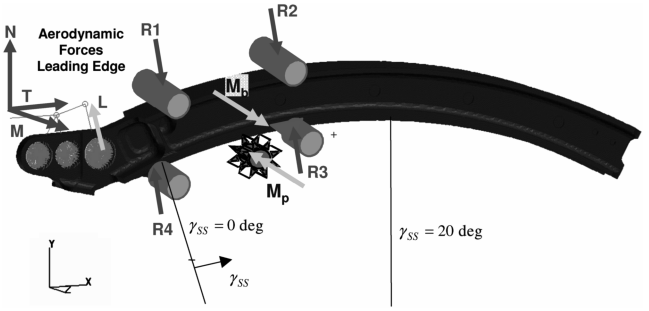


**Fig. 4 Kinematics boundary conditions for varying slat-track position $\gamma_{SS}$.**

to allow a sufficiently wide range of exploration of the response of the structure in the standard normal space. Subsequently, a least-squares response surface [38] (RS) was created to approximate and predict the response of the structure without requiring a full analysis.

The use of response surfaces can be prone to errors, however, especially for reliability problems [39]. In fact, in this type of analysis, the correct approximation of the limit-state function (LSF) in the stochastic space is essential. Even a small error in the estimation can cause a considerable variation in the approximation of the probability of failure due to the nonlinear relation between the reliability index $\beta$ and the standard normal cumulative distribution function $\Phi$ (see [9] for a more detailed explanation). Thus, a careful check of the validity of the models was carried out (see Sec. V.A).

### D. Performance Function Selection

Following the previous considerations, the choice of the performance function $G$ for the reliability analysis and optimization is related to the desired minimum safety factor. For the slat track, a safety-factor minimum value of 2.5 was selected. The performance function can then be written as

$$\text{safety factor} = 2.5 \Rightarrow G = \text{safety factor} - 2.5 \tag{2}$$

With this choice, the $G$ function is positive where the safety factor is larger than 2.5.

The threshold value of 2.5 for the safety factor was selected because it is close to the minimum value for the safety factor observed during the DOE, which constitutes the domain of validity of the RS. In the case that a wider sampling interval for the DOE is possible, the RS can be validated on a larger domain, thus allowing the selection of a lower threshold.

The probabilistic constraint of Eq. (1) can thus be written

$$P(G < 0) = P(\text{safety factor} < 2.5) = 9.86 \times 10^{-10} \tag{3}$$

## V. Results

### A. Design Exploration

The results of the design exploration are reported here. The range of exploration of the system response was from $-15\sigma$ to $+15\sigma$ for each input parameter, and a Latin hypercube DOE strategy was selected. This strategy is similar to random sampling, with the difference that the $N$ samples put in the $n$-dimensional space are placed in subsets of equal probability, thus yielding a more uniform distribution of the samples based on the probability density [40]. The results for the difference-thickness and the difference-base-height parameters were reported in terms of safety factor and total mass and can be seen in Figs. 5 and 6. For the two remaining variables (difference inner top height and difference top height) the distribution of the samples in terms of the safety factor and total mass is very similar to the distribution of the samples for difference base height, and thus they were not reported.

It can be seen from Fig. 5 that the relation between the safety factor and the input parameters is not the same for all of them. Particularly, a variation of the difference-thickness parameter (defined as the

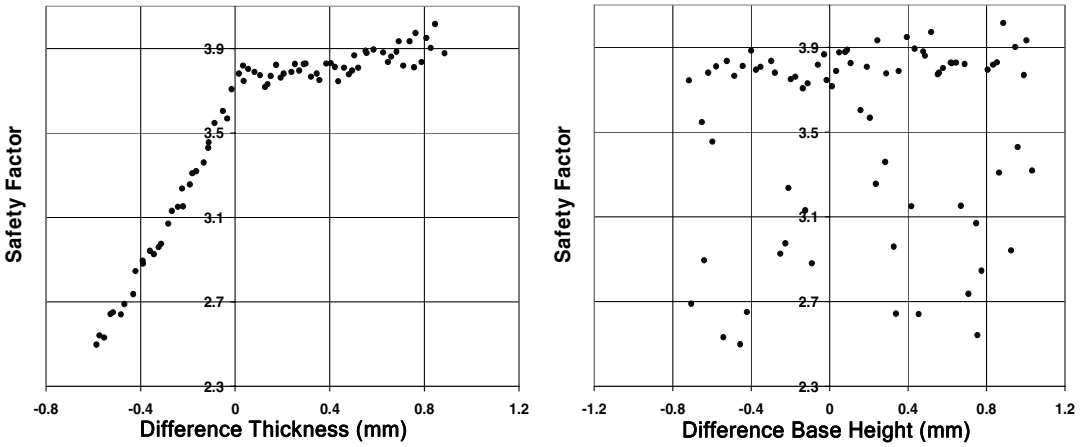


**Fig. 5 Results of the Latin hypercube DOE for the safety factor vs the difference thickness and the difference-base-height parameters.**

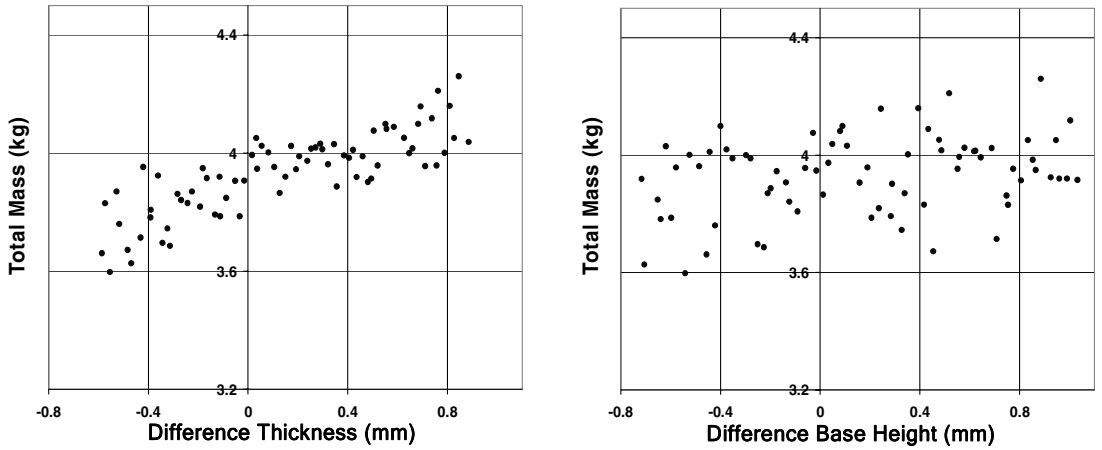


**Fig. 6 Results of the Latin hypercube DOE for the total mass vs the difference thickness and the difference-base-height parameters.**

difference between the actual and the nominal value) determines two different samples populations in the safety factor. In fact, if the difference-thickness parameter is negative, the approximate slope of the population is steeper than the case in which the difference-thickness parameter is positive. This shows that the sensitivity coefficient of the safety factor changes considerably with respect to a variation of the difference-thickness parameter. Moreover, the scatter of the two populations due to the variation of the other parameters is small. This means that the dependency between the difference-thickness parameter and the safety factor is not significantly influenced by the variation of other parameters.

To better explain the behavior of the system response shown in Fig. 5, a careful analysis of the values of the safety factor on the FE model was done. In particular, the identification of the elements for which the safety factor assumes the minimum values (also called hot spots) was carried out. Because the performance of the system is represented by the minimum value of the safety factor, the location of the first hot spot also identifies the element of the FE mesh for which this minimal value occurs. The analysis revealed that the first hot spot for which the safety factor is minimal changes depending on the value of the difference thickness, as defined in Sec. II.A. The different locations of the first hot spots for the cases of negative and positive difference thickness (with respect to the nominal value) are shown in Fig. 7.

In fact, when the difference-thickness parameter is positive, the predominant hot-spot location (for the first and the other hot spots) is the one shown in Fig. 7b. When the difference-thickness parameter decreases, a new predominant location can be identified that is more sensible than the first one to variations of the difference-thickness parameter. This new location is shown in Fig. 7a. This explains why

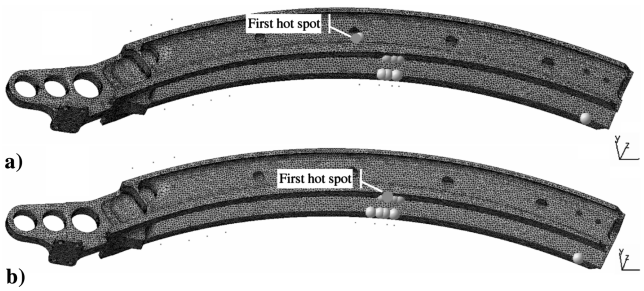


**Fig. 7 Location of the first hot spot for a) negative difference thickness and b) positive difference thickness.**

the scatter plot of Fig. 5 shows a population of samples with two different linear behaviors. This was taken into account in the response-surface calculation process, as explained later.

On the other hand, the behavior for the total mass is smoother than the safety factor, and for all the parameters there is only a small linear correlation. This is logical, because mass depends linearly on geometrical dimensions.

The results of the DOE were used to build two response surfaces, one for the safety factor and one for the total mass. To model the dependency of the safety factor from the difference-thickness parameter with sufficient accuracy, an optimal RS model [38,41] (O-RSM) procedure was carried out to find an optimal selection of terms for a least-squares model within the DOE domain of exploration of the input parameters. In this procedure, for a given set of simulated data pairs $(x^i, y^i)$ $(i = 1, \ldots, N)$, an iterative process $x^i \in \Re^n$ is

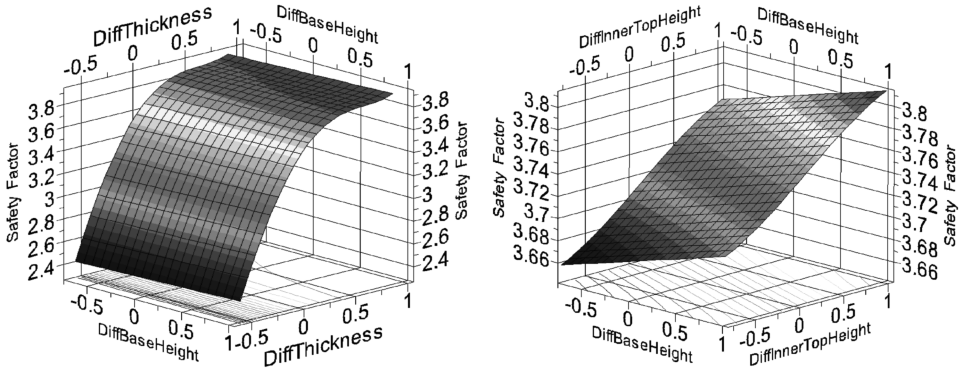


**Fig. 8 Sections of the response model for the safety factor.**

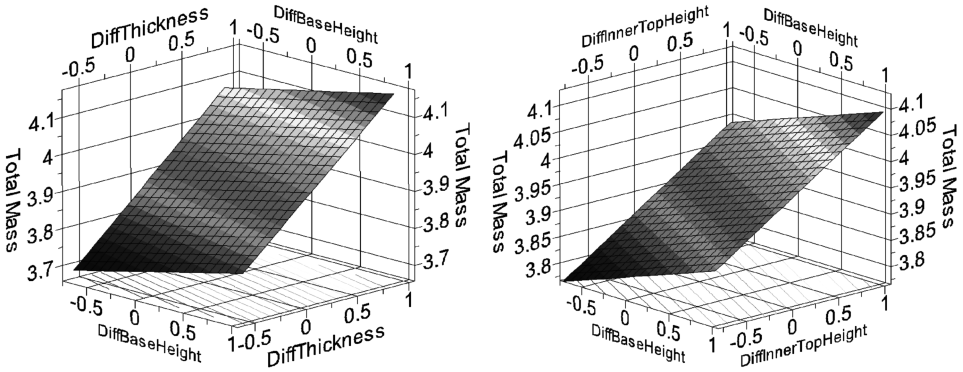


**Fig. 9 Sections of the response model for the total mass.**

carried out to find the basis $B_j(x)$ $(j = 1, \ldots, m)$ of functions defined in $\Re^n \to \Re$ and the set of coefficients $\alpha_1, \ldots, \alpha_m$ that, given the linear fitting function

$$y(x; \alpha_1, \ldots, \alpha_m) = \sum_{j=1}^{m} \alpha_j B_j(x) \tag{4}$$

minimizes the sum

$$\sum_{i=1}^{N} [y^i - y(x^i; \alpha_1, \ldots, \alpha_m)]^2 \tag{5}$$

For the safety factor, the selected basis $B_j(x)$ of functions was a third-order polynomial with first-order sine and cosine functions. The resulting fitting function showed to be more suitable to efficiently model the special correlation between the difference-thickness parameter and the safety factor, while also keeping a good accuracy for the other parameters. Some sections of the model are shown in Fig. 8.

For the total mass, the selected response model was a quadratic Taylor polynomial with a strong prevalence of linear terms over quadratic terms, which well represents the computed samples (see Fig. 9).

The analytical expressions and the coefficients of the two response models are shown in Tables 3 and 4. For each response model, quality indexes were computed to verify the fitting and prediction accuracy within the limits of the domain of definition of the models. In particular, three regression parameters were computed: $R^2$, $R^2_{\text{adj}}$, and $R^2_{\text{press}}$. Values of $R^2$ and $R^2_{\text{adj}}$ close to 1 mean that the model well fits the values of the simulation points used to calculate the model, whereas values of $R^2_{\text{press}}$ close to 1 indicate that the model will perform well for points that were not simulated. In particular, $R^2_{\text{press}}$ is an index of the predictive capability of the model within the definition domain. Further details on the definition of these parameters and their properties can be found in [38,39].

The quality indexes for the safety-factor and the total-mass models are reported in Table 5.

### B. Statistical Characterization of the Performance Function

To assess the effect of the introduced variability on the system response, a probabilistic characterization of the performance function (see Sec. IV.D) for the original design point was carried out. Using the response surface, a Monte Carlo simulation of 5000 samples was used to estimate the mean and the standard deviation. The limited sample size was sufficient for the convergence of the estimator of the statistical moments. The population obtained was then analyzed with a least-squares procedure using a histogram representation to find the best probabilistic density model that represents the population distribution. It was found that the response of the system follows an extreme type III of the smallest values (also known as the Weibull of the minimum values) distribution [13], as shown in Fig. 10, with a mean of 1.235, standard deviation of 0.041, skewness of −0.501, and kurtosis of 0.36. This model was verified with an $\chi^2$ hypothesis test [13], which checks that the selected model is representative of the data set used for the least-squares procedure.

**Table 3 Terms and coefficients of the response model for the safety factor**

| Term | Coefficient |
|---|---|
| DiffBaseHeight | $2.301 \times 10^{-2}$ |
| DiffTopHeight | $-4.661 \times 10^{-2}$ |
| sin (DiffTopHeight) | $8.804 \times 10^{-2}$ |
| cos (DiffTopHeight) | $3.647 \times 10^{-2}$ |
| sin (DiffInnerTopHeight) | $6.518 \times 10^{-2}$ |
| DiffThickness | $5.608 \times 10^{-1}$ |
| cos (DiffThickness) | 3.700 |
| $\text{DiffThickness}^2$ | 1.146 |
| $\text{DiffThickness}^3$ | $1.802 \times 10^{-1}$ |
| DiffThickness × DiffTopHeight × DiffInnerTopHeight | $2.957 \times 10^{-2}$ |

**Table 4 Terms and coefficients of the response model for the total mass**

| Term | Coefficient |
|---|---|
| 1 | 3.930 |
| DiffBaseHeight | $5.393 \times 10^{-2}$ |
| DiffThickness | $1.908 \times 10^{-2}$ |
| DiffTopHeight | $4.509 \times 10^{-2}$ |
| DiffInnerTopHeight | $1.108 \times 10^{-1}$ |
| DiffBaseHeight$^2$ | $7.128 \times 10^{-5}$ |
| DiffBaseHeight × DiffThickness | $-2.271 \times 10^{-3}$ |
| DiffBaseHeight × DiffTopHeight | $-3.496 \times 10^{-5}$ |
| DiffBaseHeight × DiffInnerTopHeight | $-1.330 \times 10^{-4}$ |
| DiffThickness$^2$ | $-6.586 \times 10^{-5}$ |
| DiffThickness × DiffTopHeight | $-3.041 \times 10^{-3}$ |
| DiffThickness × DiffInnerTopHeight | $2.275 \times 10^{-4}$ |
| DiffTopHeight$^2$ | $-3.041 \times 10^{-4}$ |
| DiffTopHeight × DiffInnerTopHeight | $1.088 \times 10^{-4}$ |
| DiffInnerTopHeight$^2$ | $-2.655 \times 10^{-4}$ |

**Table 5 Quality indexes of the response models for the safety factor and the total mass**

| | $R^2$ | $R^2_{adj}$ | $R^2_{press}$ |
|---|---|---|---|
| Safety-factor model | 0.9860 | 0.9841 | 0.9806 |
| Total-mass model | 0.9999 | 0.9999 | 0.9999 |

### C. Reliability Analysis

After the statistical characterization of the performance function, a reliability analysis using the reliability index approach [16] was carried out. The response models computed for the safety factor and the total mass were used as metamodels to assess the reliability of the slat-track structure.

The reliability analysis step is necessary to find the position of the most probable point (MPP) on the LSF in the standard normal space [19]. The distance between the MPP location and the design origin in the standard normal space (reliability index $\beta$) represents a measure of the possible improvement of the design parameters that can be gained with the reliability-based optimization procedure using a $6\sigma$ target (see Sec. V.D).

The results of the reliability analysis procedure are reported in Table 6 and shown in Fig. 11. The reliability analysis results of the nominal point are as follows: 7 iterations, 52 LSF evaluations, and the reliability index was 14.398. The starting point is the nominal design, characterized by the mean values of the input parameters.

To better explain the results of the MPP location in Table 6, a negative value in the standard normal space means that the mean value should be reduced by the amount specified in standard deviation units. Thus, the value is relative to the origin of the standard normal space, which is the nominal point (mean values). Thus, the results expressed in the parameters space (second row of Table 6) are the new mean values of the difference between the design values and the mean manufacturing values (see Sec. II.A for the definition of the input parameters).

### D. Reliability-Based Design Optimization

The results of the optimization process for the analysis case are reported in this section. The target of the optimization is to reduce the total mass while keeping a distance of $6\sigma$ from the region of the event space in which the safety factor has a value equal to or smaller than 2.5. This means that the newly found design will have, given the scatter in the input parameters, a probability of $9.86 \times 10^{-10}$ of having a safety factor smaller than 2.5.

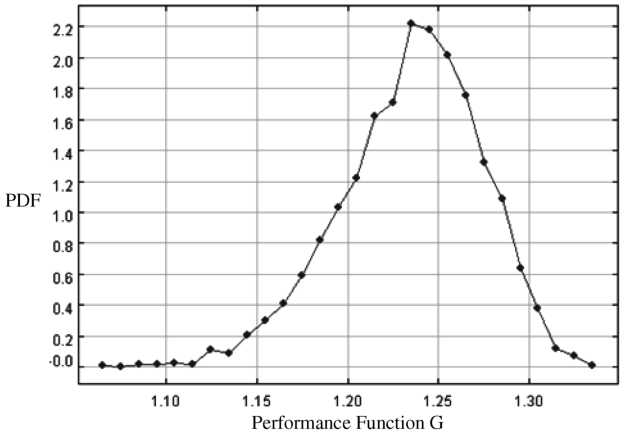


**Fig. 10 Probability density function of the MCS population of the performance function *G*.**

To carry out the RBDO process, a two-step strategy was adopted. In the first step, a standard deterministic optimization procedure is performed to efficiently find a point located on the limit-state function $G$ that minimizes the total mass of the structure. At this stage, no probabilistic constraint is taken into account and the point found has a probability of failure of approximately 0.5 (see Figs. 12 and 13). In the second step, another optimization procedure is started from the deterministic optimum point to find the probabilistic optimum point, which satisfies the probabilistic constraint.

An alternative one-step procedure can also be used. In this approach, the probabilistic constraint is enforced from the first optimization step. As a consequence, the probability of failure for each step of the optimization procedure has to be assessed to check that the probabilistic constraint is not violated. It is clear that in some situations, this methodology could require a much higher number of computations with regard to the two-step approach, which is usually undesirable and computationally expensive. In particular, experience showed that the two-step approach is particularly useful when the MPP for the nominal design is located at a distance of $\beta > 1.5 \times \beta_t$ (e.g., the target reliability index $\beta_t$ is $6\sigma$ and the reliability index of the current nominal design $\beta$ is $12\sigma$). In this case, in fact, the optimization iterations that would require the evaluation of the probabilistic constraint would be limited to the second part of the optimization that pulls the optimum point to a distance of $\beta_t = 6\sigma$ (for the present case) from the deterministic one and that usually requires less iteration steps. This is demonstrated in Figs. 14 and 15.

In this case, in fact, if the probabilistic constraint would have been considered in only one single optimization procedure (instead of two) starting from the nominal point, the number of evaluations required to enforce the constraint would require a much high number of performance function evaluations. This approach constitutes an acceptable compromise between performance and accuracy.

For both optimization procedures, each input parameter was constrained to a range of $-15\sigma$ to $+15\sigma$, which is also the range of validity of the RSM and avoids extrapolation.

The results of the deterministic optimization are shown in Fig. 12. The optimization procedure required 11 SQP iterations and a total of 59 LSF evaluations to converge. The main result of the deterministic optimization was a reduction of the total mass from 3.9327 to 3.5446 kg.

The second optimization process was carried out using the performance measure approach and the enhanced hybrid-mean-

**Table 6 Location of the most probable point in the standard normal space ($\sigma$ coordinate) and in the parameter space**

| Difference base height | Difference thickness | Difference top height | Difference inner top height |
|---|---|---|---|
| $-1.3586\sigma$ | $-14.324\sigma$ | $-0.3000\sigma$ | $-0.4330\sigma$ |
| 0.0714 mm | −0.5639 mm | 0.1856 mm | 0.0250 mm |

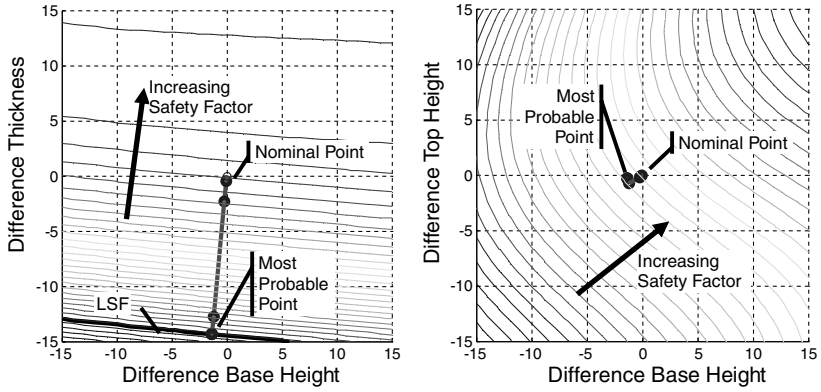


**Fig. 11 Results of the reliability analysis procedure; location of the most probable point in the standard normal space.**

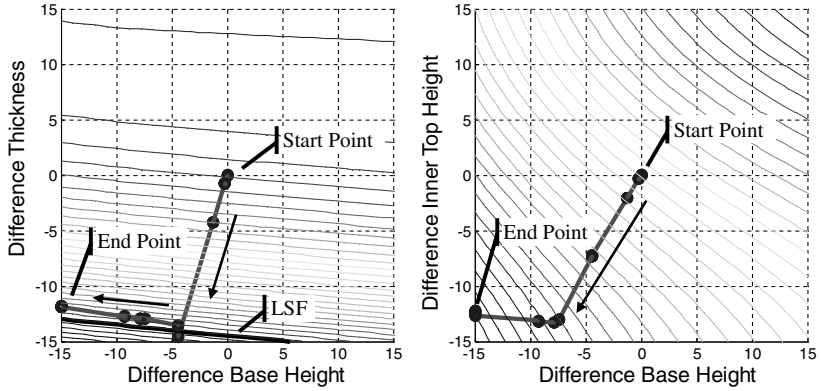


**Fig. 12 Deterministic optimization procedure in the standard normal space *Y*.**

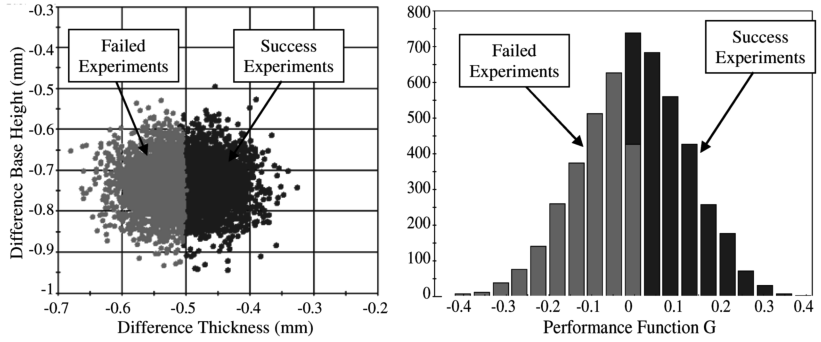


**Fig. 13 Reliability of the deterministic optimal point.**

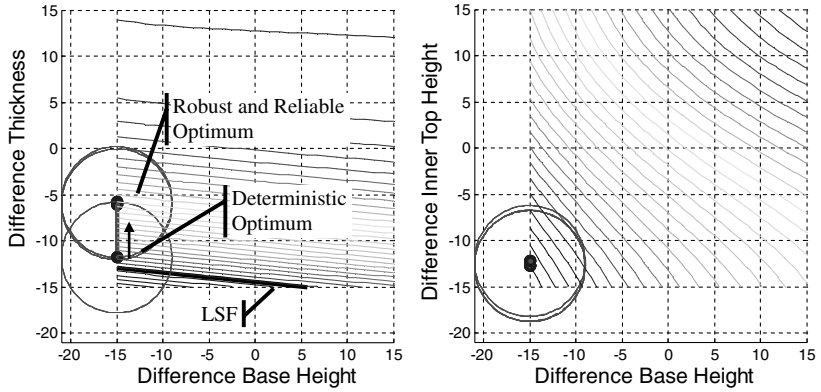


**Fig. 14 RBDO results in the standard normal space.**

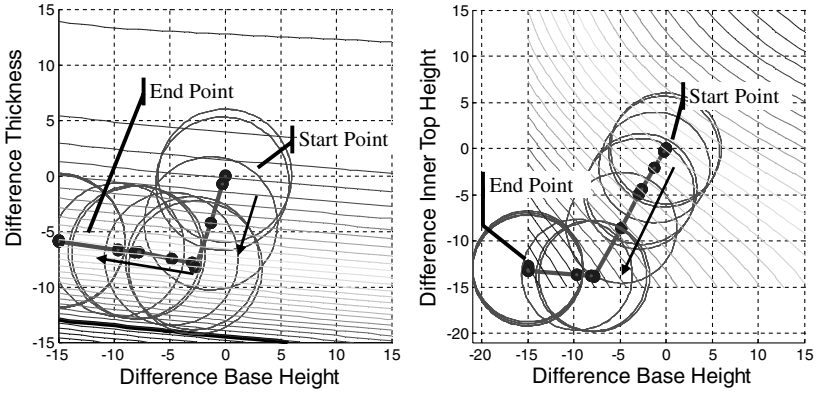


**Fig. 15 Full RBDO procedure results in the standard normal space.**

value method (HMV+) algorithm [42], looking for a reliable optimum. The results of the optimization are shown in Fig. 14. The reliability-based optimization procedure required two SQP iterations and a total of 280 LSF evaluations to converge. The main result of this optimization was a slight increase of the total mass from 3.5446 to 3.6236 kg.

To demonstrate the efficiency gain for this two-step optimization strategy, a complete optimization loop starting from the nominal design point and taking into account the probabilistic constraint was carried out. This optimization procedure required 13 SQP iterations with approximately 985 limit-state evaluations, which is 2.9 times more than the actual effort spent with the two-step approach. For the sake of completeness, this one-step full process is shown in Fig. 15.

The reliability-based optimization results clearly show that in terms of standard deviation, there is room for improvement of the design while keeping the same reliability.

The design found with the reliability-based design optimization [which was placed at $6\sigma$ for the RBDO algorithm using the enriched performance measure approach (PMA+) with HMV+ [42]) shows a mass reduction with respect to the nominal design. This is demonstrated in Table 7. In particular, a negative value in the last row of Table 7 (final optimization point) indicates that the mean values of the parameters reported in Table 1 can be reduced.

The mass reduction of 7.86% constitutes the main result of the optimization. This reduction is particularly significant when one considers that the standard deviations observed in the measured tolerance data are very small.

Further reduction of the mass can be achieved by sampling a wider interval of variation of the input parameters (see Sec. V.A for the used parameters' range). However, an increased interval of exploration of the system response may require taking into account other failure modes (e.g., the buckling of the left and right thin plates for which the difference-thickness parameter is defined) that were not relevant for the present case. In this paper, these additional failure modes were not considered in the analysis, because their effect was negligible on the estimation of the probability of failure for the selected range of variation of the design parameters. Nevertheless, attention should be given to avoid that the estimation of the reliability of the structure is affected by other failure modes not included in the analysis and that might become as relevant as those considered for the reliability analysis [12]. In this view, the mass reduction results obtained can be considered valid, because in the selected range of variation of the input parameters, other failure modes are not relevant. However, this is not always the case and a careful check should always be carried out.

It is important to note that the time needed for the reliability analysis and the optimization process was very limited, due to the use of the response-surface model. In fact, each FE computation of the structural and durability analysis takes a total of 40 min on a standard PC, whereas the response surface takes less than a second to evaluate. This makes it very clear that a Monte Carlo simulation and the optimization process would have been much more expensive, in terms of computational effort and time, without the use of a response model. Moreover, the total effort of the optimization process can be further reduced by using improved optimization techniques, as described in [28].

The integration of the reliability optimization together with the precise manufacturing process used for the slat track thus opens the way for more reliable and lightweight products, while still preserving a very reliable safety margin in the design.

## VI. Conclusions

In this paper, a slat track under variable load conditions was analyzed considering the variabilities in the input parameters. Several observations were made.

In a traditional design process, it is not possible to assess the effect of variability on durability performance. As compensation, safety factors are introduced that, unfortunately, may lead to slightly overdesigned structures. For the slat track, variabilities of the geometric tolerances for four parameters were considered. These tolerances were parameterized as shape design variables using mesh morphing technology, enabling the accurate assessment of their effect on the durability performance. The entire process (mesh morphing, finite element analysis, durability analysis, reliability assessment, and optimization) was captured in a state-of-the-art process integration and design optimization environment. A design of experiments with response-surface methodology was used to speed up the calculation process. A moderate range of variation of the design parameters was selected, because the paper concerned an assessment and optimization on an already manufactured, extensively tested, and validated slat track (and not on a novel design concept for which much larger ranges of variation could be of interest).

**Table 7 Results for the two optimization procedures and mass reduction summary**

| | Difference base height, mm | Difference thickness, mm | Difference top height, mm | Difference inner top height, mm | Total mass, kg | Safety factor | Reliability index |
|---|---|---|---|---|---|---|---|
| Nominal point | 0.1518 | 0.1472 | 0.0250 | 0.1027 | 3.9327 | 3.7373 | 14.398 |
| Deterministic optimum | −0.7359 | −0.5044 | −1.0267 | −0.8099 | 3.5446 | 2.5001 | 0.0 |
| Probabilistic optimum | −0.7359 | −0.2076 | −1.0267 | −0.8099 | 3.6236 | | 6.0 |
| | | | *Mass reduction* 7.86% | | | | |

A statistical characterization of the selected parameters was done using measured data during the production process, thus enabling the use of reliability analysis techniques. The performance function for the reliability analysis was based on the safety-factor prediction of the durability computation. The safety factor was somewhat lowered when compared with the nominal design, but still quite a high value was used to absolutely guarantee the design safety.

Furthermore, state-of-the-art reliability-based design optimization methods (using the enriched performance measure approach with the enhanced hybrid mean value) were used to take advantage of the margin in the reliability: the design could be relocated in the parameters space to a point at which a lighter structure is possible, while still guaranteeing a design reliability of $6\sigma$. More specifically, for the slat track, a mass reduction of 7.86% with respect to the nominal mass was obtained. This is a very significant result of the optimization, especially when one considers that the standard deviations observed in the measured tolerance data are very small. Further gain in the mass reduction can be achieved if a different setup of the morphing transformation is created and other input parameters are introduced in the design process. Also, attention should be given that other failure modes (e.g., buckling) do not become as relevant as the failure mode considered.

## Acknowledgments

The support of the European Commission and the Instituut voor Innovatie door Wetenschap en Technologie (IWT) is gratefully acknowledged.

## References

[1] Jans, J., Wyckaert, K., Brughmans, M., Kienert, M., Van der Auweraer, H., Donders, S., and Hadjit, R., "Reducing Body Development Time by Integrating NVH and Durability Analysis from the Start," SAE 2006 World Congress, Detroit, MI, Society of Automotive Engineers, Paper 2006-01-1228, Apr. 2006.

[2] Van der Auweraer, H., Tournour, M., Wyckaert, K., and De Langhe, K., "Vibro-Acoustic CAE from an Industrial Application Perspective," SIAT 2005 Conference, Pune, India, Society of Automotive Engineers, Paper 2005-26-050, Jan. 2005.

[3] Bäcker, M., Langthaler, T., Olbrich, M., and Oppermann H., "The Hybrid Road Approach For Durability Loads Prediction," Society of Automotive Engineers, Paper 2005-01-0628, 2005.

[4] Van der Auweraer, H., and Leuridan, J., "The New Paradigm of Testing in Today's Product Development Process," *International Conference on Noise and Vibration Engineering (ISMA 2004)* [CD-ROM], Katholieke Univ. Leuven, Leuven, Belgium, Sept. 2004, pp. 1151–1170.

[5] Oberkampf, W. L., Diegert, K. V., Alvin, K. F., and Rutherford, B. M., "Variability, Uncertainty and Error in Computational Simulation," *AIAA/ASME Joint Thermophysics and Heat Transfer Conference*, Vol. 357-2, Heath Transfer Div., American Society of Mechanical Engineers, New York, 1998, pp. 259–272.

[6] Zang, T. A., Hemsch, M. J., Hilburger, M. W., Kenny, S. P., Luckring, J. M., Maghami, P., Padula, S. L., and Stroud, W. J., "Needs and Opportunities for Uncertainty-Based Multidisciplinary Design Methods for Aerospace Vehicles," NASA TM-2002-211462, 2002.

[7] Oberkampf, W., DeLand, S. M., Rutherford, B. M., Diegert, K. V., and Alvin, K. F., "Error and Uncertainty in Modeling and Simulation," *Reliability Engineering and System Safety*, Vol. 75, No. 3, 2002, pp. 333–357. doi:10.1016/S0951-8320(01)00120-X

[8] Oberkampf, W., DeLand, S. M., Rutherford, B. M., Diegert, K. V., and Alvin, K. F., "Estimation of Total Uncertainty in Modeling and Simulation," Sandia National Labs., Rept. SAND2000-0824, Albuquerque, NM, Apr. 2000; reprint, Apr. 2005.

[9] Melchers, R. B., *Structural Reliability Analysis and Prediction*, 2nd ed., Wiley, New York, 1999.

[10] Der Kiureghian, A., "First and Second Order Reliability Methods," *Engineering Design Reliability Handbook*, CRC Press, Boca Raton, FL, 2005.

[11] Thoft-Christensen, P., "System Reliability," *Engineering Design Reliability Handbook*, CRC Press, Boca Raton, FL, 2005.

[12] Ba-abbad, M. A., Kapania, R. K., and Nikolaidis, E., "Reliability-Based Structural Optimization of an Elastic-Plastic Beam" *AIAA Journal*, Vol. 41, No. 8, Aug. 2003, pp. 1573–1582.

[13] Montgomery, D. C., and Runger, G. C., *Applied Statistics and Probability for Engineers*, Wiley, New York, 1994.

[14] Erto, P., *Probabilità e Statistica per le Scienze e l'Ingegneria*, 2nd ed., McGraw–Hill, New York, 2003.

[15] Der Kiureghian, A., and Liu, P.-L., "Optimization Algorithms for Structural Reliability Analysis," Univ. of California, Berkeley, Rept. UCB/SESM-86/09, Berkeley, CA, 1986.

[16] Sudret, B., and Der Kiureghian, A., "Stochastic Finite Element Methods and Reliability: A State of the Art Report," Department of Civil and Environmental Engineering, Univ. of California, Rept. UCB/SEMM-2000/08, Berkeley, CA, Nov. 2000.

[17] Youn, B. D., Choi, K. K., and Park, Y. H., "Hybrid Analysis Method for Reliability-Based Design Optimization," *Journal of Mechanical Design*, Vol. 125, June 2003, pp. 221–232. doi:10.1115/1.1561042

[18] Youn, B. D., Choi, K. K., and Du, L., "Adaptive Probability Analysis Using An Enhanced Hybrid Mean Value Method," *Structural and Multidisciplinary Optimization*, Vol. 29, No. 2, 2005, pp. 134–148. doi:10.1007/s00158-004-0452-6

[19] D'Ippolito, R., Donders, S., Tzannetakis, N., Van der Auweraer, H., and Vandepitte, D., "Integration of Probabilistic Methodology in the Aerospace Design Optimization Process," 1st AIAA Multidisciplinary Design Optimization Specialist Conference, Austin, TX, AIAA Paper 2005-2137, Apr. 2005

[20] D'Ippolito, R., Donders, S., Tzannetakis, N., Van de Peer, J., and Van der Auweraer, H., "An Overview of Limit State Algorithms and Their Applicability to Finite Element Reliability Analysis," *Safety and Reliability of Engineering Systems and Structures (ICOSSAR'05)* [CD-ROM], Millpress, Rotterdam, The Netherlands, June 2005.

[21] Schuëller, G. I., Pradlwarter, H. J., and Koutsourelakis, P. S., "A Critical Appraisal of Reliability Estimation Procedures for High Dimensions," *Probabilistic Engineering Mechanics*, Vol. 19, No. 4, pp. 463–474. doi:10.1016/j.probengmech.2004.05.0042004.

[22] D'Ippolito, R., Hack, M., Donders, S., Van der Auweraer, H., Tzannetakis, N., Farkas, L., and Desmet, W., "Robust and Reliable Fatigue Design of Automotive and Aerospace Structures," Fatigue 2007 (to be published).

[23] Donders, S., d'Ippolito, R., Van der Auweraer, H., Hack, M., Tzannetakis, N., Farkas, L., and Desmet, W., "Uncertainty-Based Design in Automotive and Aerospace Engineering," SAE 2007 World Congress, Detroit, MI, Society of Automotive Engineers, Paper 2007-01-0355, Apr. 2007.

[24] Schueremans, L., "State of the Art Report: Structural Reliability in Design and Analysis," Katholieke Univ. Leuven, Leuven, Belgium, Mar. 2003.

[25] Mourelatos, Z., and Liang, J., "A Reliability-Based Robust Design Methodology," SAE World Congress, Detroit, MI, , Society of Automotive Engineers, Paper 2005-01-0811, Apr. 2005.

[26] D'Ippolito, R., Hack, M., Donders, S., and Hermans, L., "A Reliability Analysis Approach to Improve the Fatigue Life of a Vehicle Knuckle," *Recent Advances in Structural Dynamics (RASD 2006)* [CD-ROM], Inst. of Sound and Vibration Research, Southampton, England, U.K., July 2006.

[27] D'Ippolito, R., Donders, S., Hack, M., Tzannetakis, N., Van der Linden, G., and Vandepitte, D., "Reliability-Based Design Optimization of Composite and Steel Aerospace Structures," 47th AIAA/ASME/ASCE/AHS/ASC Structures, Structural Dynamics, and Materials Conference, Newport, RI, AIAA Paper 2006-2153, May 2006.

[28] Ba-abbad, M. A., Nikolaidis, E., and Kapania, R. K., "New Approach for System Reliability-Based Design Optimization," *AIAA Journal*, Vol. 44, No. 5, May 2006, pp. 1087–1096.

[29] Schlesinger, S., "Terminology for Model Credibility," *Simulation*, Vol. 32, No. 3, 1979, pp. 103–104. doi:10.1177/003754977903200304

[30] "Guide for the Verification and Validation of Computational Fluid Dynamics Simulations," AIAA Rept. G-077-1998, Reston, VA, Jan. 1998.

[31] OPTIMUS, Software Package, Ver. 5.2, Noesis Solutions NV, Leuven, Belgium, Aug. 2006.

[32] Van der Auweraer, H., Van Langenhove, T., Brughmans, M., El Masri, N., and Olbrechts, T., "Advanced Mesh Based Design Optimization for Early-Stage Virtual Prototyping," *International Conference on Noise and Vibration Engineering (ISMA 2004)* [CD-ROM], Katholieke Univ. Leuven, Leuven, Belgium, Sept. 2004.

[33] Bosmans, I., Brughmans, M., Brizzi, P., Shiozaki, H., and Yanase, J., "Application of Morphing in Concept Phase of Vehicle Development," 2005 JSAE Annual Congress, Japan Society of Automotive Engineers, Paper 2005-5475, May 2005.

[34] Barkey, M., Hack, M., Speckert, M., Zingsheim, F., and Schäfer, G., "LMS.FALANCS Theory Manual," LMS Deutschland, Kaiserslautern, Germany, 2002.
[35] Vecchio, A., Carmine, R., de Voghel, R., Van der Linden, G., and Guillaume, P., "Numerical Evaluation of Damage Distribution over a Slat Track Using Flight Test Data," *Proceedings of IMAC XXI* [CD-ROM], Society for Experimental Mechanics, Bethel, CT, 2003.
[36] LMS Virtual.Lab, Software Package, Ver. 6B, LMS International, Leuven, Belgium, Nov. 2006.
[37] Lorenzen, T. J., and Anderson, V. L., *Design of Experiments, A No-Name Approach*, Marcel Dekker, New York, 1993.
[38] Myers, R. H., and Montgomery, D. C., *Response Surface Methodology: Process and Product Optimization Using Designed Experiments*, Wiley, New York, 1995.
[39] Bucher, C., and Macke, M., "Response Surfaces for Reliability Assessment," *Engineering Design Reliability Handbook*, CRC Press, Boca Raton, FL, 2005.
[40] Olsson, A., Sandberg, G., and Dahlblom, O., "On Latin Hypercube Sampling for Structural Reliability Analysis," *Structural Safety*, Vol. 25, No. 1, 2003, pp. 47–68. doi:10.1016/S0167-4730(02)00039-5
[41] Lawson, C. L., and Hanson, R. J., *Solving Least-Squares Problems*, SIAM, Philadelphia, 1995.
[42] Tu, J., and Choi, K. K., "A New Study on Reliability Based Design Optimization," *Journal of Mechanical Design*, Vol. 121, No. 4, 1999, pp. 557–564.

J. Samareh
*Associate Editor*